Disease Models & Mechanisms 3, 785-798 (2010) doi:10.1242/dmm.005447

RESEARCH ARTICLE

Disease-specific, neurosphere-derived cells as models for brain disorders

Nicholas Matigian[1,*], Greger Abrahamsen[1,*], Ratneswary Sutharsan[1], Anthony L. Cook[1], Alejandra M. Vitale[1], Amanda Nouwens[2,3], Bernadette Bellette[1], Jiyuan An[1], Matthew Anderson[1], Anthony G. Beckhouse[1], Maikel Bennebroek[1], Rowena Cecil[1], Alistair M. Chalk[1], Julie Cochrane[1], Yongjun Fan[1], François Féron[1,‡], Richard McCurdy[1,§], John J. McGrath[1,4,5], Wayne Murrell[1,¶], Chris Perry[1,6], Jyothy Raju[1], Sugandha Ravishankar[1], Peter A. Silburn[1,7], Greg T. Sutherland[1], Stephen Mahler[2], George D. Mellick[1], Stephen A. Wood[1], Carolyn M. Sue[1,8], Christine A. Wells[1] and Alan Mackay-Sim[1,**]

SUMMARY

There is a pressing need for patient-derived cell models of brain diseases that are relevant and robust enough to produce the large quantities of cells required for molecular and functional analyses. We describe here a new cell model based on patient-derived cells from the human olfactory mucosa, the organ of smell, which regenerates throughout life from neural stem cells. Olfactory mucosa biopsies were obtained from healthy controls and patients with either schizophrenia, a neurodevelopmental psychiatric disorder, or Parkinson's disease, a neurodegenerative disease. Biopsies were dissociated and grown as neurospheres in defined medium. Neurosphere-derived cell lines were grown in serum-containing medium as adherent monolayers and stored frozen. By comparing 42 patient and control cell lines we demonstrated significant disease-specific alterations in gene expression, protein expression and cell function, including dysregulated neurodevelopmental pathways in schizophrenia and dysregulated mitochondrial function, oxidative stress and xenobiotic metabolism in Parkinson's disease. The study has identified new candidate genes and cell pathways for future investigation. Fibroblasts from schizophrenia patients did not show these differences. Olfactory neurosphere-derived cells have many advantages over embryonic stem cells and induced pluripotent stem cells as models for brain diseases. They do not require genetic reprogramming and they can be obtained from adults with complex genetic diseases. They will be useful for understanding disease aetiology, for diagnostics and for drug discovery.

INTRODUCTION

Most clinical disorders arise from multiple gene-environment interactions rather than variations in single genes (Wray et al., 2008) – a particularly important concept when considering neurological conditions and psychiatric disorders. Even many 'single gene' diseases do not manifest in all carriers of a mutation, indicating that other factors can be involved (Summers, 1996). This complexity brings into focus the need to find new models to identify the complex genetic and environmental interactions that contribute to brain disorders. Of paramount importance, the field requires pragmatic methods that can readily derive large numbers of relevant cells from multiple cases and controls, which are needed to represent the spectrum of variability between individuals. Accessible non-neural cells like skin fibroblasts or transformed lymphocytes have been used to identify differences in cell biology associated with schizophrenia (SZ) and Parkinson's disease (PD) (Mahadik and Mukherjee, 1996; Miyamae et al., 1998; Winkler-Stuck et al., 2004; Hoepken et al., 2008) but the utility of non-neural cells for understanding the cellular bases of neurological and neuropsychiatric disorders is limited (Matigian et al., 2008). Another approach is to develop stem cell models of disease: embryonic stem (ES) cells carrying genetic mutations have been isolated after pre-implantation genetic diagnosis (Verlinsky et al., 2005; Mateizel et al., 2006), and induced pluripotent stem (iPS) cells have been generated from patients, including those with PD (Park et al., 2008). However, major challenges remain in applying these models to the study of sporadic brain diseases, as the models must be routine and robust as well as informative for the disease process.

The olfactory mucosa, the organ of smell in the nose, is a neural tissue that is accessible in human adults (Féron et al., 1998) and demonstrates disease-dependent alterations in cell biology in Alzheimer's disease, Rett syndrome, fragile X syndrome and SZ (Wolozin et al., 1992a; Abrams et al., 1999; Féron et al., 1999; Arnold et al., 2001; Ronnett et al., 2003; McCurdy et al., 2006). The olfactory sensory neurons are replaced by neurogenesis that continues throughout adult life from stem cells on the basement membrane

[1]National Centre for Adult Stem Cell Research, Eskitis Institute for Cell and Molecular Therapies, Griffith University, Brisbane, QLD 4111, Australia
[2]Australian Institute for Bioengineering and Nanotechnology, The University of Queensland, St Lucia, QLD 4072, Australia
[3]School of Chemistry and Molecular Biosciences, The University of Queensland, St Lucia, QLD 4072, Australia
[4]Queensland Centre for Mental Health Research, The Park Centre for Mental Health, Wacol, QLD 4076, Australia
[5]Queensland Brain Institute, The University of Queensland, St Lucia, QLD 4072, Australia
[6]Department of Otolaryngology Head and Neck Surgery, Princess Alexandra Hospital, Woolloongabba, QLD 4102, Australia
[7]School of Medicine, The University of Queensland, St Lucia, QLD 4072, Australia
[8]Kolling Institute of Medical Research, The University of Sydney, Royal North Shore Hospital, St Leonards, NSW 2065, Australia
*These authors contributed equally to this work
‡Present address: Neurobiologie des Interactions Cellulaires et Neurophysiopathologie (CNRS UMR 6184), Université de la Méditerranée (Aix-Marseille II), Faculté de Médecine Nord, Institut Fédératif de Recherche Jean Roche (IFR11), Marseille, France
§Present address: University of Pennsylvania Medical Center, Department of Psychiatry, Translational Research Labs, 125 South 31st Street, Philadelphia, PA 19104-3403, USA
¶Present address: Institutt for Kirurgisk Forskning, Sognsvannsveien 20, Rikshospitalet HF 0027 Oslo, Norway
**Author for correspondence (a.mackay-sim@griffith.edu.au)

(Mackay-Sim and Kittel, 1991; Leung et al., 2007). Olfactory mucosa contains stem cells that are multipotent and can be propagated as stem or progenitor cells in neurospheres, a hallmark of neural stem cells (Roisen et al., 2001; Murrell et al., 2005; Murrell et al., 2008; Murrell et al., 2009). They can be proliferated in vitro and differentiated into multiple cell types including neurons and glia (Roisen et al., 2001; Murrell et al., 2005; Murrell et al., 2008; Murrell et al., 2009).

With evidence for disease-related alterations in olfactory epithelium and the loss of olfaction that is associated with many neurological diseases, including SZ and PD (Brewer et al., 2003; Doty, 2009; Haehner et al., 2009; Turetsky et al., 2009), we hypothesized that olfactory mucosal stem cells derived from SZ and PD patients would provide an accessible, proliferating population to investigate the cellular bases of these diseases (Mackay-Sim and Silburn, 2008). We predicted that olfactory neurosphere-derived (ONS) cells would exhibit disease-specific alterations in these two unrelated neurological and neuropsychiatric disorders: SZ, a highly heritable neurodevelopmental condition (Raedler et al., 1998), and PD, a neurodegenerative disease that is heritable in only about 5% of familial cases (Lesage and Brice, 2009). We examined and compared ONS cells from multiple patients with SZ and PD to identify aspects of cell biology that were shared by each group of patients and different from healthy controls.

We report here that ONS cells from SZ and PD patients, when subjected to gene and protein expression profiling and cell function assays, revealed different signalling pathways altered in each patient group, compared with healthy controls. In SZ ONS cells we predicted and found alterations in cell signalling pathways involved in cell proliferation, neurogenesis and cell adhesion (Féron et al., 1999; McCurdy et al., 2006), whereas skin fibroblasts from the same patients did not show these altered pathways. In PD ONS cells we predicted and found convergence on molecular pathways previously associated with this disorder – namely, mitochondrial function, oxidative stress and xenobiotic metabolism (Henchcliffe and Beal, 2008). These results demonstrate that the ONS cell model is robust and informative, with the potential for providing a new tool for studying the mechanisms of human brain disorders and diseases.

RESULTS

We undertook multiple experiments on the 42 ONS cell lines from patients and controls (SZ, *n*=9; PD, *n*=19; control, *n*=14). We characterized the phenotype using flow cytometry on a subset of 18 cell lines (SZ, *n*=6; PD, *n*=6; control, *n*=6). As experimental controls we also characterized fibroblasts from control patients (*n*=9). Gene expression profiling compared all 42 ONS cell lines from patients and controls. Protein expression profiling compared nine ONS cell lines (*n*=3 for each group). Gene and protein expression profiling was confirmed on two replicate samples of each cell line, each grown independently. Gene expression differences were validated for subsets of genes using quantitative reverse-transcriptase polymerase chain reaction (qRT-PCR). Protein expression was validated by western blot analysis for one protein in protein samples from nine ONS cell lines. Pathway analysis of

Table 1. qRT-PCR confirmation of microarray expression data for selected genes

		Illumina		qPCR	
Gene symbol	**GenBank**	***P* value**	**Fold change**	***P* value**	**Fold change**
Schizophrenia					
AXIN2	NM_004655	0.0153	2.05	0.4690	1.38
CDH2	NM_001792	0.0009	–2.37	0.0350	–2.17
GSK3B	NM_002093	0.0280	–1.20	0.0320	–1.28
ITGA8	NM_003638	0.0013	6.93	0.0140	6.65
ITGB1BP1	NM_022334	0.0459	1.92	0.8590	1.04
PIK3R1	NM_181504	0.0035	1.35	0.5200	1.09
PPP2R2B	NM_181676	0.0026	–4.26	0.9260	–1.08
WNT5A	NM_003392	0.0002	2.07	0.0170	1.94
RGS4	NM_005613	0.0014	–2.93	0.0070	–4.59
GABRE	NM_021990	0.0005	1.92	0.0090	1.75
LRP8	NM_033300	0.0329	–1.53	0.3450	–1.30
SLC1A1	NM_004170	0.0053	–2.43	0.0300	–2.38
PARVB	NM_001003828	0.0010	–1.44	0.6910	–1.08
LAMA3	NM_198129	0.0021	1.94	0.0100	2.50
RELN	NM_005045	0.0130	–4.15	0.0430	–8.33
Parkinson's disease					
GABBR2	NM_005458	0.0006	4.99	0.0140	3.41
GSTM1	NM_000561	0.0011	–7.46	0.0720	–5.92
MGST1	NM_020300	0.0059	–1.82	0.0470	–1.69
PSG4	NM_002780	0.0041	5.42	0.0010	11.73

Comparison of relative gene expression using qRT-PCR to confirm microarray expression levels. Transcripts for re-analysis were selected from those significantly differentially expressed between patient and controls on the microarray across a range of fold-change differences, with a minimum fold-change difference of 1.2. Fold-change and *P* values show patient samples relative to control samples. Fold-change differences were in the same direction in qRT-PCR as on the microarray. qRT-PCR was undertaken on mRNA from the same samples used for the microarray analysis.

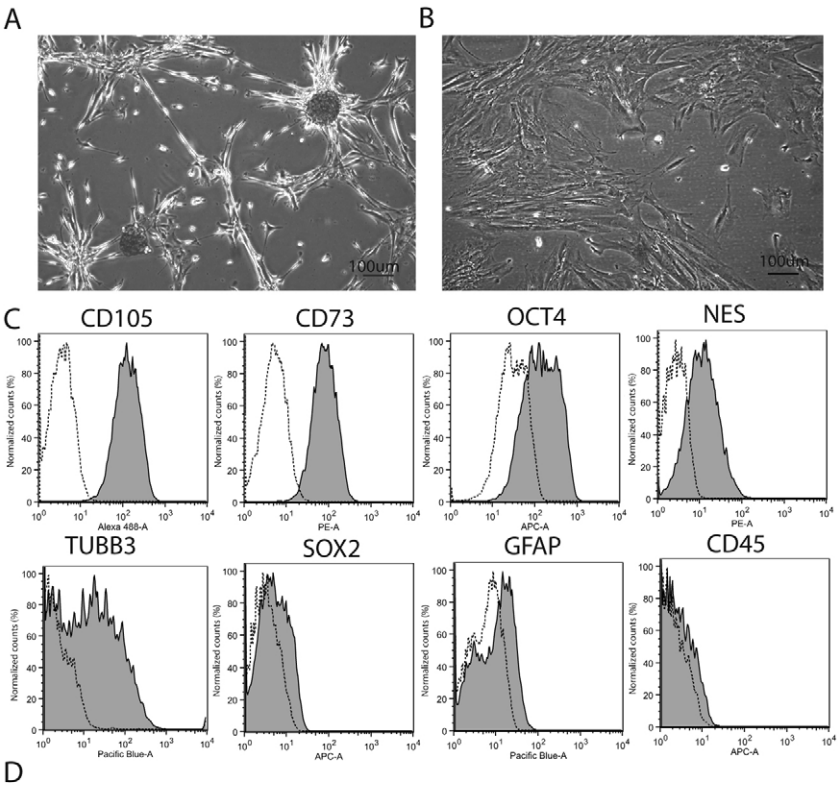

D

Marker	Control % Positive cells +/- SEM	N	Sz % Positive cells +/- SEM	N	PD % Positive cells +/- SEM	N
CD105	98.7±0.4	6	99.6±0.1	5	93.6±1.5	6
CD73	81.9±16	6	99.1±0.2	5	93.8±5.5	6
OCT4	40.8±4.7	6	55.2±3.6	5	61.6±4.5	6
NES	28.8±7.2	6	42.2±9.1	6	45.9±10.5	5
TUBB3	35.0±5.9	6	22.8±2.0	6	34.1±1.5	5
SOX2	<1%	6	<1%	6	<1%	5
GFAP	<1%	6	<1%	6	<1%	5
CD45	<1%	6	<1%	5	<1%	6

Fig. 1. Phenotype of ONS cells. (A) Olfactory neurospheres being formed from cells cultured from biopsy of human olfactory mucosa, grown in serum-free medium containing EGF and FGF2. (B) Cells grown from dissociated olfactory neurospheres in a medium containing serum; these are 'olfactory neurosphere-derived' (ONS) cells. (C) Typical flow cytometry results from an ONS cell line, plotting the relative frequency of cells labelled (*y*-axis) against fluorescence intensity (*x*-axis) for each of the antibodies (name above panel; antibody-labelled cells in grey; isotype-control cells in white). (D) Summary data for all ONS cells from patients and controls. Positive cells are those with antibody fluorescence greater than isotype controls.

the differentially expressed genes and proteins was undertaken using two independent databases: one public and one commercially available. Assays of six metabolic functions were performed on SZ and control ONS cells (n=9 for each group), and on PD and control ONS cells (n=14 and 16, respectively). Thus, the disease-specific differences in cell biology were observed across multiple patients and multiple ONS cell lines for each disease.

Growth, morphology and immunophenotype of ONS cells

ONS cells are derived from neurospheres that form when dissociated olfactory mucosal cells are grown in a serum-free medium containing epidermal growth factor (EGF) and fibroblast growth factor 2 (FGF2) (Fig. 1A). Neurospheres were generated from all 42 patients and controls, with no obvious disease-related differences in neurosphere growth and formation. The neurospheres were dissociated and grown in the presence of serum as an adherent monolayer of ONS cells (Fig. 1B). For ONS cells, the fastest growth occurs between 10 to 60 days in vitro (up to passage 12). At passage 4 (20 days in vitro) the doubling time of nine control cell lines was 28.3±1.4 hour. All the experiments here were undertaken on cells at passages 4-8 (up to 40 days in vitro). We checked chromosomal stability by karyotyping 22 olfactory cell lines at passages 3-10: all were normal. Two ONS cell lines were grown continuously for more than 160 days in vitro, through at least 16 passages. Each cell line reached 95% of its total growth in 60 days (12 passages) and divided only very slowly after 100 days. We checked gene expression stability in one cell line from passages 7-25. At passages 10, 13, 16, 19, 22 and 25 the gene expression profile (across the 10,000 expressed genes) was correlated with the gene expression profile at passage 7, yielding correlation coefficients of 0.99, 0.98, 0.98, 0.96, 0.94 and 0.94, respectively. This high level of correlation indicates that ONS cells are quite stable genetically for many passages and more than 100 days in vitro.

Flow cytometric analysis indicated some heterogeneity in immunophenotype of the cells in ONS cultures (Fig. 1C,D). The majority of cells were immunopositive with antibodies to CD105 and CD73. Antibodies to nestin (NES) and OCT4 labelled many fewer cells at low intensity than did those against CD105 and CD73. All these proteins are used as markers for other stem cell phenotypes (CD105 and CD73 for mesenchymal stem cells; NES

for neural stem cells; OCT4 for ES cells). The cells were immunopositive for β-tubulin III (TUBB3), a marker for neural progenitors and developing neurons, but not immunopositive for SOX2 and several proteins associated with more-differentiated phenotypes (GFAP, CD45). Analysis of variance indicated significant differences between groups (P<0.05) for CD105 and OCT4, and significant pair-wise differences between SZ and PD for CD105 and TUBB3, and between control and PD cells for OCT4. Gene expression profiling (below) further described the phenotype of these cells and the differences between them.

SZ-derived ONS cells displayed altered neurodevelopmental genes, pathways and function

We used microarray gene expression profiling to test our hypothesis that we would identify convergent, dysregulated neurodevelopmental processes in ONS cells from patients with SZ. We observed profound and highly reproducible differences in the transcriptomes of SZ and control ONS cells. Of the 10,515 probes detected on the microarrays of the SZ and control ONS cells, 16% (1700) were differentially expressed [P<0.05 (Benjamini and Hochberg multiple testing adjusted P values); supplementary material Table S1; experiments performed in duplicate]. An equal number of the genes were overexpressed or underexpressed in SZ ONS cells compared with control cells, and 12% (219/1702) were expressed in SZ cells at least twofold more, or less, than in control cells. Fifteen genes that were differentially expressed on the microarrays were validated using qRT-PCR and showed differences between patients and controls (SZ, n=9; control, n=9) consistent with the original array findings. These differences were statistically significant in 9/15 of the transcripts tested by qRT-PCR (Table 1).

We asked whether differentially expressed genes represented multiple members of any cell signalling pathways that could coordinately alter cell function in SZ. Pathway analysis is a statistical test of the number of differentially expressed genes that contribute to known cell signalling pathways. For SZ our prediction was that the differentially expressed genes would be over-represented in cellular pathways of neurodevelopment. Pathway convergence was assessed using Ingenuity Pathway Analysis, which identified ten pathways that were significantly over-represented (P<0.01; Table 2). A second analysis using the public database DAVID identified five pathways that were significantly over-represented (P<0.01; Table 2). Both methods of pathway analysis identified the same essential dysregulation of highly interconnected functions involved in brain development through the processes of focal adhesion, axonal guidance and receptor-mediated signalling (supplementary material Fig. S1). Importantly, five of the pathways identified are already implicated in SZ ('Reelin signalling in neurons', 'VDR/RXR activation', 'IL-8 signalling', 'Glutathione metabolism', 'ErbB signalling').

We next looked at differences in protein expression in a subset of patient-derived cells lines (n=3 per group). Proteomic analysis using two-dimensional dye-in-gel-electrophoresis (2D-DIGE) identified 20 proteins whose expression was significantly altered in ONS cells from SZ patients compared with controls (P<0.05; experiments performed in duplicate; Fig. 2). There was a convergence between gene and protein expression (Table 3). Of the proteins with significantly altered expression, transgelin 2 (TAGLN2) was selected for western analysis, which confirmed this protein was reduced in the SZ cell lines compared with controls (supplementary material Fig. S3).

Table 2. Cellular signaling pathways altered in schizophrenia

	Count	*P* value
Ingenuity Pathway Analysis (gene expression)		
Ephrin receptor signaling	28	0.00003
NRF2-mediated oxidative stress response	26	0.0003
Axonal guidance signaling	43	0.001
IL-8 signaling	23	0.002
Virus entry via endocytic pathways	14	0.003
Semaphorin signaling in neurons	10	0.006
Fcγ receptor-mediated phagocytosis in macrophages and monocytes	14	0.006
Glutathione metabolism	10	0.007
Reelin signaling in neurons	12	0.008
VDR/RXR activation	12	0.009
DAVID analysis (gene expression)		
Ribosome	21	0.000002
Focal adhesion	38	0.0001
Axon guidance	25	0.001
ErbB signaling pathway	18	0.004
Inactivation of GSK3 by AKT causes accumulation of β-catenin in alveolar macrophages	9	0.008
Ingenuity Pathway Analysis (protein expression)		
Glycolysis/gluconeogenesis	4	0.00001

Molecular pathways significantly altered in SZ identified by Ingenuity Pathway Analysis and DAVID analysis from the 1700 genes and 20 proteins with significantly altered expression in SZ cells compared with controls. Pathways are identified statistically using Fisher's exact test to calculate a probability (P value) of finding the number of genes or proteins on the differentially expressed list (Count) compared with the number of molecules in the pathway and the total numbers of genes or proteins sampled.

With the set of functional assays, we demonstrated that the SZ-derived ONS cells had significantly increased caspase-3/7 activity, an indicator of apoptosis (P=0.028; Fig. 3F). Although this neurodevelopmental function was altered, there were no differences from control ONS cells in a range of other metabolic function assays (Fig. 3). There was no correlation between the results obtained in any functional assays and age (r^2 range 0.00009-0.0722) or cell-line passage number (r^2 range 0.0002-0.063).

In order to test whether the ONS model offers an advantage over other somatic cells, we next examined the gene expression of skin fibroblasts obtained from the same SZ patients as the ONS cells. Relatively few (118) transcripts were differentially expressed between patient and control fibroblast lines (P<0.05; supplementary material Table S2). Of these, none was altered twofold or greater. Ingenuity Pathway Analysis showed no convergence on the pathways identified in the ONS transcriptome. Two molecular pathways were significantly over-represented in SZ fibroblasts compared with control fibroblasts ('Hypoxia signalling in the cardiovascular system', P=0.006; 'Riboflavin metabolism', P=0.009) but the representation of differentially expressed genes in each pathway was low: only three and two molecules, respectively. We

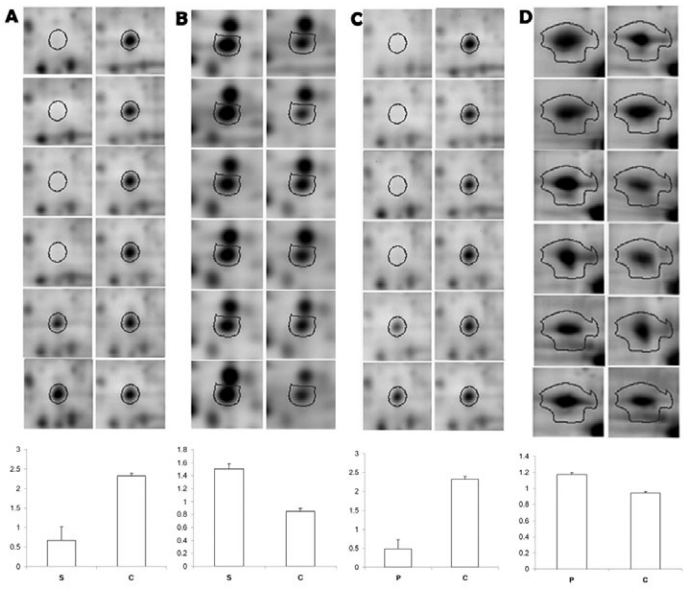

Fig. 2. Examples of differentially expressed proteins. Each pair of columns compares protein spots in 2D-DIGE gels from three patients and three controls. Images of spots from two gels per individual, using Cy3 dye and Cy5 dye, are illustrated consecutively for each of three individuals per group in each column. Each pair of columns represents patients on the left and controls on right. The graphs below show normalized spot volume for each of the spots shown above (mean ± s.e.m.). Lines drawn on gels indicate the regions over which spot volume was calculated. Spots were normalized to intensity of same spot identified in a mixture of proteins from all cells, run in the same gel and imaged using Cy2 dye. (A) GSTO1 is underexpressed in SZ (P=0.001). (B) STMN1 is overexpressed in SZ (P=0.001). (C) GSTO1 is underexpressed in PD (P=0.001). (D) P4HB is overexpressed in PD (P=0.002).

Table 3. Protein and gene expression in Schizophrenia and Parkinson's disease

	Protein expression		mRNA expression	
Gene symbol	Fold change	*P* value	Fold change	*P* value
Schizophrenia				
ABI1	−2.3	0.01	1.13	0.01
ACTB	−1.3	0.0004	−1.09	0.005
DPYSL2	−1.6	0.02	−1.06	0.43
ESD	−2.6	0.04	1.07	0.13
GAPDH	−1.35	0.003	−1	0.95
GSTO1	−2.8	0.001	−1.01	0.96
HNRNPA1	1.45	0.01	1.21	0.26
LMNA	−1.3	0.02	1.03	0.74
P4HA1	−1.3	0.01	1.01	0.97
PGAM1	−1.35	0.001	−1.11	0.33
PGK1	−1.55	0.001	−1.13	0.23
STMN1	1.85	0.0003	−1.26	0.31
TAGLN	−1.6	0.01	−1.12	0.005
TAGLN2	−1.5	0.02	−1.19	0.06
TPI1	−1.35	0.03	−1.07	0.38
TPM1	−1.85	0.01	−1.33	0.02
TPM2	−1.55	0.01	−1.05	0.05
TRA1	1.2	0.02	1.01	0.89
TTN	1.45	0.03	1.06	0.67
UCHL1	1.7	0.03	−1.01	0.99
Parkinson's disease				
ANXA4	−1.2	0.04	1.05	0.64
CNN1	2.1	0.01	1.35	0.43
DPYSL2	−1.2	0.04	−1.12	0.06
GSTO1	−3.7	0.0006	−1.04	0.65
LMNA	−1.2	0.04	−1.04	0.51
NQO1	−1.9	0.0002	−1.31	0.02
P4HA2	1.4	0.01	1.26	0.01
P4HB	1.2	0.03	1.03	0.65
PGK1	−1.2	0.02	1.12	0.32
UCHL1	2.5	0.01	−1.51	0.18
VCP	1.2	0.03	−1.01	0.93

Genes whose protein expression was differentially expressed in SZ and PD compared with the level of gene expression measured by mRNA expression. Relative protein expression (patient vs control) was quantified with 2D-DIGE in replicate in two independent samples from three patients from each group and three controls. Relative mRNA expression was quantified on the Illumina BeadArray with ONS cells from 42 patients and controls in two independent samples. 'Fold-change' and '*P* values' show patient samples relative to samples from healthy controls.

conclude that skin fibroblasts are not informative compared with ONS lines generated from the same patient-control cohort.

PD-derived ONS cells displayed altered metabolic genes, pathways and functions

PD provides an obvious clinical contrast to SZ, on many levels. It was predicted that we would identify different convergent, dysregulated metabolic processes in ONS cells from patients with PD. Again, we found profound differences in the transcriptomes of PD and control ONS cells. Five percent of the probes (514/10300) were significantly differently expressed in PD compared with control cells (P<0.05; supplementary material Table S3). An equal number of genes were overexpressed or underexpressed in PD ONS cells compared with control cells, and 8% (43/514) were expressed in PD cells at least twofold more, or less, than in controls. Four genes that were differentially expressed on the microarrays were selected for verification of expression using qRT-PCR (PD, n=19; control, n=13) and a high level of agreement was found between the qRT-PCR and microarray results (Table 1).

Pathway analysis using Ingenuity Pathway Analysis and DAVID identified eight cell pathways that were significantly over-represented among the differentially expressed transcripts (P<0.01; Table 4). Our prediction was that PD cells would demonstrate differences in mitochondrial function, oxidative stress and xenobiotic metabolism. This was borne out by significant over-representation of genes in highly inter-connected pathways, including four involved in oxidative stress and xenobiotic metabolism ('NRF2-mediated oxidative stress response', 'Aryl hydrocarbon receptor signalling', 'Glutathione metabolism', 'Xenobiotic metabolism signalling'; supplementary material Fig. S2), exemplified by the significant downregulation of glutathione transferases (*GSTM1*, *MGST1*) in the PD cells (Table 1).

Independent examination of proteins expressed in three ONS cell lines derived from PD patients revealed 11 proteins that were

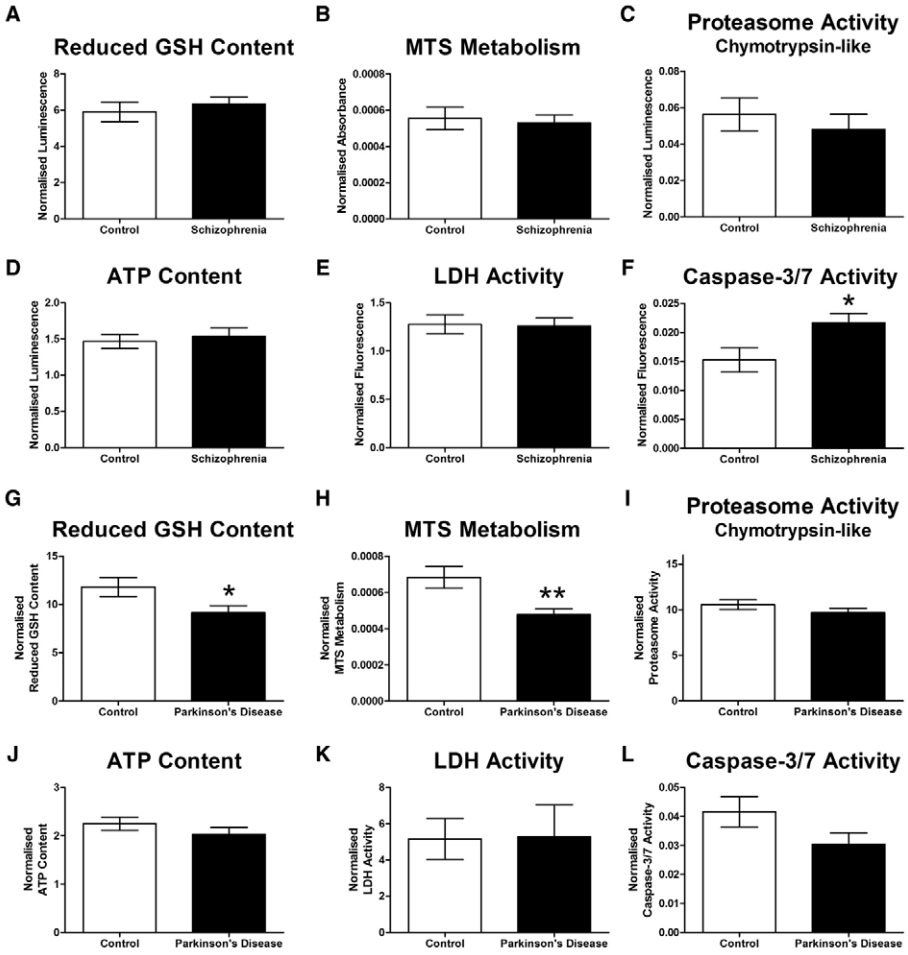

Fig. 3. Functional assays of ONS cells. (A-F) SZ versus control. All assays were performed on the same cells: SZ, black bars (n=9); control, white bars (n=9). Caspase-3/7 activity was significantly increased in SZ (P=0.023). (G-L) PD versus control. All assays were performed on the same cells: PD, black bars (n=14); control, white bars (n=16). Reduced GSH (glutathione) content was significantly decreased (P=0.042). MTS metabolism was significantly reduced (P=0.007).

significantly altered compared with controls (Table 3). Western analysis showed TAGLN2 protein was expressed more in PD ONS cells compared with controls (supplementary material Fig. S3). As with SZ ONS cells, there was agreement between protein and transcriptome expression. This agreement was further evident in the Ingenuity Pathway Analysis of the proteins, which identified four pathways that overlapped with the pathways identified from the gene expression analysis (Table 4). Proteomic and gene expression pathways clearly converged on oxidative stress and metabolic pathways in the ONS cells derived from PD patients.

We examined the metabolic function assays of the ONS cells from PD patients to validate our predictions of abnormal oxidative function, and confirmed these disease-associated differences in cell function assays (Fig. 3). The PD cells demonstrated significant reductions in glutathione (reduced glutathione content, P=0.042; Fig. 3G) and metabolic activity (MTS metabolism, P=0.007; Fig. 3H). There was no correlation between the results obtained in any functional assay and age (r^2 range 0.0004-0.04) or cell line passage number (r^2 range 0.0006-0.2).

DISCUSSION

We show here that human olfactory neurosphere-derived cell lines (ONS cells) demonstrate alterations in gene expression, protein expression and cell function, including dysregulated neurodevelopmental pathways in SZ and dysregulated mitochondrial function, oxidative stress and xenobiotic metabolism in PD. These disease-specific differences conform to current broad hypotheses about the aetiologies of these diseases but also provide specific candidate genes and cell pathways for future investigation. Human ONS cells therefore provide informative cellular models for SZ and sporadic PD. By contrast, fibroblasts from SZ patients and healthy controls showed few gene expression differences, confirming our previous observations (Matigian et al., 2008).

Diseases like SZ and sporadic PD are difficult to model because of the complex interactions between uncertain environmental exposures and unknown genetic risk factors. To address this, accessible cells like lymphocytes and skin fibroblasts have been used to identify patient-control differences. For SZ and PD these differences have been modest, perhaps because these cell types do not reflect tissue-specific differences important for brain function (Matigian et al., 2008; Wang et al., 2009). As a neural tissue, the olfactory mucosa might be more relevant, as demonstrated previously by disease-associated differences in cell functions (Wolozin et al., 1992a; Féron et al., 1999; McCurdy et al., 2006) and tissue structure (Arnold et al., 2001; Ronnett et al., 2003). ONS cells provide new patient-derived, stem-cell-based models of neurological disease that are accessible in all adults and provide new routes for understanding the pathogenesis of complex diseases.

They can be grown in standardized conditions, frozen, banked, thawed, and regrown in quantity for gene and protein expression analyses and functional investigations.

It is expected that susceptibility to disease-risk environmental exposures in SZ and PD is related to the genetic background of cases compared with controls. This study confirmed the hypothesis that patients would share a common set of altered cellular pathways and gene networks that could lead to a disease phenotype in ONS cells. These models provide opportunities for investigating the effects of environmental exposures on cells of different genetic background to further understand gene-environment interactions in SZ and PD.

Patient-derived ONS cells provide disease-relevant findings even in a relatively undifferentiated state. For this study we grew the ONS cells in standard culture conditions to obtain enough for mRNA, protein and functional analyses as a baseline for future studies of differentiated cells. ONS cells might be even more informative when differentiated into specific neural lineages (Murrell et al., 2005; Murrell et al., 2008; Murrell et al., 2009). Because of their accessibility and relative ease of generation it should be feasible to grow ONS cells from enough patients to investigate cellular sequelae of clinical subtypes (e.g. tremor-dominant or non-dominant PD). ONS cells are a potentially unlimited source of renewable patient-derived cells for the development of new diagnostics and high-throughput drug screening.

Table 4. Cellular signaling pathways altered in Parkinson's disease

	Count	*P* value
Ingenuity Pathway Analysis (gene expression)		
NRF2-mediated oxidative stress response	13	0.0002
Aryl hydrocarbon receptor signaling	11	0.0003
Glutathione metabolism	7	0.0003
Purine metabolism	16	0.002
Arginine and proline metabolism	7	0.002
LPS/IL-1-mediated inhibition of RXR function	11	0.004
Xenobiotic metabolism signaling	13	0.004
Neuropathic pain signaling in dorsal horn neurons	7	0.007
DAVID analysis (gene expression)		
Glutathione metabolism	8	0.0003
Purine metabolism	13	0.004
Ingenuity Pathway Analysis (protein expression)		
NRF2-mediated oxidative stress response	3	0.0003
Hypoxia signaling in the cardiovascular system	2	0.001
Arginine and proline metabolism	2	0.001
Aryl hydrocarbon receptor signaling	2	0.005

Molecular pathways significantly altered in PD identified by Ingenuity Pathway Analysis and DAVID analysis from the 514 genes and 11 proteins with significantly altered expression in PD cells compared with controls. Pathways are identified statistically using Fisher's exact test to calculate a probability (*P* value) of finding the number of genes or proteins on the differentially expressed list (Count) compared with the number of molecules in the pathway and the total numbers of genes/proteins sampled.

Technical considerations

Human olfactory sensory neurons are continually regenerated throughout life (Murrell et al., 1996) from stem or progenitor cells in the olfactory epithelium (Chen et al., 2004; Leung et al., 2007). Olfactory neuroblasts (Wolozin et al., 1992b) and neurospheres (Roisen et al., 2001; Murrell et al., 2005) can be grown from the human olfactory mucosa. In the present study, olfactory neurospheres were generated from olfactory mucosa biopsies by growing the dissociated cells in serum-free medium containing EGF and FGF2. Olfactory neurospheres produced in this way contain multipotent progenitor cells capable of differentiating into cells of the neural lineage (Roisen et al., 2001; Murrell et al., 2005; Othman et al., 2005) and multiple other cell types (Murrell et al., 2005). Neurosphere-derived cells are generated by dissociating neurospheres and propagating the cells in a serum-containing medium as an adherent monolayer. In this medium, human ONS cells shared many characteristics with, but were not identical to, bone-marrow stromal cells, including sharing many surface antigens and expressed genes (Delorme et al., 2010). In the present study, flow cytometric analysis revealed low or absent levels of expression of the neural stem or progenitor markers NES and TUBB3 (low) and SOX2 (absent), with negligible expression of the astrocyte marker GFAP. They expressed high levels of two cell-surface markers of bone-marrow stromal or stem cells, CD73 and CD 105, and a low level of expression of a pluripotency marker, OCT4. The ONS cells from patients and controls were similar in morphological and immunological phenotype, consistent with an 'ecto-mesenchymal' stem or progenitor cell population (Delorme et al., 2010). Despite this relatively undifferentiated state, the ONS cells demonstrated significant disease-related differences. These differences might be magnified or altered if the ONS cells were differentiated into the relevant cells of the nervous system (Murrell et al., 2005), and this ability to differentiate demonstrates their advantage over other adult-derived cells such as fibroblasts and lymphoblasts. In this sense, the current study provides a baseline for future studies of differentiated cells derived from ONS cells.

Although we favour the hypothesis that genetic background is the major contributor to the disease-related differences we observed, they might be caused in total or in part by epigenetic alterations brought about by the disease process or by therapeutic drugs. Without pre- and post-diagnosis samples these issues cannot be resolved. We consider epigenesis unlikely because the patients received a variety of combinations of medications and doses and we found no significant effects of medication on gene expression or cell function. Additionally, the negligible patient-control difference in fibroblast gene expression suggests that systemic disease effects or systemic drug effects are minimal, at least in SZ. One cannot rule out tissue-specific effects that might manifest in ONS cells. The patient and control groups were not exactly matched for sex and age. This might have biased the results for the PD sample because the 14 controls included some age- and sex-matched to the SZ patients.

The reliability of the gene and protein expression data was verified in several ways. Gene expression was independently verified using qRT-PCR for selected mRNAs, and protein expression was verified by western analysis of one protein in independent ONS cell samples. The concordance between mRNA

and protein levels provides counter-verification. The corresponding mRNAs for 21 (68%) proteins were overexpressed or underexpressed in the same direction, and six of these differences (19%) were statistically significant ($P \leq 0.05$) for both mRNA and protein. This level of concordance between mRNA and protein expression falls within the expected modest correlation reported in other cells, varying between 20% and 70% (Chen et al., 2004; Nie et al., 2006; Pascal et al., 2008).

ONS cells as a model for SZ

SZ is considered a disorder in which brain development is altered by genetic and environmental factors (Harrison, 1999; Marenco and Weinberger, 2000; Lewis and Levitt, 2002; McGrath et al., 2003b). The current data provide numerous lines of evidence for altered molecular pathways that are involved in neurodevelopment, including cell proliferation, adhesion, migration and cell death. Importantly, several pathways confirm multiple independent observations in SZ. Of particular note are four genes – *RELN, RGS4, ERBB3* and *GSK3B* – whose expression was downregulated in ONS cells from SZ patients. There is consistent and repeatable evidence that gene and protein expression of these four genes are downregulated in post-mortem brain from SZ patients (Impagnatiello et al., 1998; Guidotti et al., 2000; Kozlovsky et al., 2000; Fatemi et al., 2001; Hakak et al., 2001; Mirnics et al., 2001; Aston et al., 2004; Kozlovsky et al., 2004; Erdely et al., 2006; Colantuoni et al., 2008). Several of these genes are involved in highly inter-related signalling pathways in which other genes are affected. GSK3β, which is downstream of neuregulin-ErbB and RELN signalling, is a potential regulator of several signalling pathways in SZ (Lovestone et al., 2007). All three pathways were significantly dysregulated in SZ ONS cells. *RELN* and the gene encoding the RELN receptor, *LRP8*, were significantly downregulated in ONS cells. RELN is an extracellular matrix protein that stabilizes neuronal microtubules to regulate neuronal migration (Hiesberger et al., 1999) and the structure of dendritic trees (Trommsdorff et al., 1999). RELN is reduced in the prefrontal cortex of humans with SZ (Impagnatiello et al., 1998). RELN binds integrin α3β1 (Schmid et al., 2005), which was also downregulated (supplementary material Table S1), suggesting a coordinated dysregulation of the RELN signalling pathway in cells from individuals with SZ, as confirmed by the pathway analysis. There is emerging evidence for dysregulated ErbB signalling in SZ (Corfas et al., 2004). ErbB3 is reduced in the prefrontal cortex in SZ (Tkachev et al., 2003) and the gene encoding its ligand, neuregulin-1 (*NRG1*), was identified in gene association studies in SZ (for a review, see Corfas et al., 2004). *ERBB3* gene expression was reduced in the SZ-derived ONS cells, and a high level of convergence from multiple molecules in the ErbB-neuregulin pathways was observed in the ONS model.

Our data direct attention to other disruptions in the highly interconnected molecular pathways affecting brain development that have not previously been implicated in SZ. The 'Ephrin signalling' pathway was the most affected pathway in ONS cells in SZ. Ephrin signalling is essential for cell and axon migration and regulates synaptic plasticity (Martinez and Soriano, 2005). In the SZ ONS cell lines the expression of three integrins was significantly altered (supplementary material Table S1) and 'Focal adhesion' was identified in the pathway analysis. A recent analysis of the 'integrin adhesome' identified 94 'intrinsic components' (Zaidel-Bar et al., 2007). Of these, 19 (20%) had altered expression in ONS cells from SZ patients.

The results provide support at a cellular level for a nexus between neurodevelopment and prenatal risk factors for SZ. First, prenatal infection by certain viruses increases the risk of SZ (Brown, 2006) and 'Virus entry via endocytotic pathways' was significantly altered in ONS cells. Second, raised maternal cytokines, including interleukin 8 (IL-8), are associated with increased risk of SZ (Brown et al., 2004), and 'IL-8 signalling' was significantly disrupted in ONS cells. Finally, reduced maternal and newborn levels of vitamin D are associated with increased risk of SZ (McGrath et al., 2003a; McGrath et al., 2004). 'VDR/RXR activation' was significantly altered in ONS cells. Involvement of VDR (the vitamin D receptor) is of interest because there is robust evidence from rodent models that reduced prenatal levels of vitamin D alter the developing and adult brain (Eyles et al., 2003; Feron et al., 2005). A plausible argument can also be made for dysregulation of retinoid signalling in the aetiology of SZ (Goodman, 1998; LaMantia, 1999), which interacts with vitamin D signalling via the retinoid X receptor (RXR). The altered pathways in ONS cells in SZ provide a plausible connection between cellular processes and susceptibilities to these environmental risks.

Skin fibroblasts are another easily accessible source of patient cells that have been used as cellular models of SZ (Mahadik and Mukherjee, 1996). Our previous observation was that fibroblasts do not show robust patient-control differences in SZ (Matigian et al., 2008). In the present study, we found small differences in gene expression in SZ fibroblasts compared with controls, with only 118 genes significantly differentially expressed, compared with 1700 in the ONS cells. Similarly, a recent study found no significant differences in gene expression and only 16 proteins differentially expressed in skin fibroblasts (Wang et al., 2009).

ONS cells as a model for PD

PD is a heterogeneous movement disorder with various degrees of tremor, rigidity and slowness of movement that has a varying age of onset. The majority of cases of PD are idiopathic, likely arising from different combinations of genetic and environmental factors (Benmoyal-Segal and Soreq, 2006). Mutations in the *PARK* genes lead to rare, familial, mendelian parkinsonism and have provided convergence on cellular processes that might be defective in all PD sufferers (Lesage and Brice, 2009). These include mitochondrial dysfunction and oxidative stress, disruption of the ubiquitin-proteasome system, and the aggregation of abnormally folded proteins such as α-synuclein (SNCA) (McNaught and Olanow, 2006). Consistent with these predictions, ONS cells derived from PD patients shared parallel dysregulation of processes involved in metabolic and oxidative stress. Crucially, many of the *PARK* genes and the identified cellular processes are interlinked. For example, several of the *PARK* gene products are located in, or can be associated with, the mitochondria (e.g. SNCA, Parkin, PINK1, DJ-1, LRRK2 and HTR2A) (Henchcliffe and Beal, 2008); others play pivotal roles in the proteasome pathway (Parkin and UCHL1) and the cellular response to oxidative stress (DJ-1, HTR2A and SNCA). These PD-associated cellular processes are targets for toxins that induce parkinsonism in animals (Jenner, 2008), and they are also implicated in toxicological effects of multiple environmental factors identified from population studies of human PD. For example,

exposure to environmental toxins such as pesticides appears to increase the risk for PD, whereas cigarette smoking and caffeine consumption are less common in patients; the impact of these risk-altering exposures is also likely to depend on an individual's genetic make-up (Mellick, 2006).

We note that the dominant signalling pathways altered in the patient-derived ONS cells in PD are interconnected and associated with mitochondrial dysfunction, oxidative stress and xenobiotic metabolism, as demonstrated in evidence from gene expression, protein expression and functional assays. Some of these pathways were identified in post-mortem studies: gene expression profiling of occipital cortex identified significant alteration in the 'NRF2-mediated oxidative stress response' pathway and similar profiling of the substantia nigra identified significant alteration in 'Aryl hydrocarbon receptor signalling' in PD (Sutherland et al., 2009). NRF2 and ARH are transcription factors that induce expression of cytoprotective genes in response to xenobiotics, including enzymes of glutathione metabolism (Denison and Nagy, 2003; Cuadrado et al., 2009), illustrating the interdependence of many of the pathways identified in the ONS cells. Further agreement with post-mortem data is the finding of significant alteration in 'Purine metabolism' that is also seen in Brodmann area 9 in PD brains (Sutherland et al., 2009). Functional analyses confirmed significant reduction in glutathione metabolism and mitochondrial function in cells from PD patients compared with controls. Additionally, ten genes with differential expression in ONS cells are also reported as up- or down-regulated in brains of PD patients compared with controls.

METHODS

Participants and nasal biopsies

All donor tissue and information were obtained with the informed consent of the participants prior to their involvement in the study and all procedures were in accordance with National Health and Medical Research Council Code of Practice for Human Experimentation, and approved by the Griffith University Human Experimentation Ethics Committee and the Wolston Park Hospital Institutional Ethics Committee. Patients with SZ (n=9) or PD (n=19) were recruited from consumer groups and through research-participant registers maintained by the Queensland Centre for Mental Health Research and the Queensland Parkinson's Project. Controls (n=14) were recruited from the general population. For the cohort of patients and controls concerning SZ, participants were interviewed with the Diagnostic Interview for Psychosis (Castle et al., 2006). In addition, the hospital records for the patients were examined in order to confirm diagnoses according to DSM IV criteria. For the cohort of patients and controls concerning PD, the patients were diagnosed according to standard clinical evaluation by a qualified neurologist with experience in movement disorders, and both patients and controls completed a questionnaire to exclude the possibility of undiagnosed PD in controls. None of the healthy controls was on psychotropic or PD medication. Details of age, medications and smoking status are given in supplementary material Table S4. The nasal biopsies were collected as an outpatient procedure as described previously (Féron et al., 1998).

Cell culture

The biopsies were initially received in cold Dulbecco's Modified Eagle Medium/Ham F-12 (DMEM/F12; JRH Biosciences) containing 10% FBS (GibcoBRL) and 1% streptomycin-penicillin (GibcoBRL). Olfactory cell suspensions were generated by digestion with dispase II (Boehringer; 2.4 units/ml, 45 minutes, 37°C) and collagenase H (Sigma; 0.25 mg/ml, 10 minutes, 37°C) accompanied by mechanical trituration, as described previously (Murrell et al., 1996; Murrell et al., 2005). The primary cultures were grown for 3 days in DMEM/F12 supplemented with 10% FBS before passaging into flasks (Nunclon) pretreated with 1 μg/cm^2 poly-L-lysine (Sigma, P6282) and culturing in DMEM/F12 containing EGF (50 ng/ml, Sigma) and FGF2 (25 ng/ml, Sigma). Neurospheres formed initially from cell clusters attached to the culture dish surface but detached when they reached about 100 μm in diameter. The free-floating neurospheres were harvested every second day from the medium change. These were dissociated with trypsin, replated at 4000 cells/cm^2 into 75 cm^2 flasks and cultured in DMEM/F12 with 10% FBS. These neurosphere-derived (ONS) cells were then expanded by passage and banked down in aliquots after harvest by storage in liquid nitrogen with 90% FBS and 10% dimethyl sulfoxide (Sigma). Frozen aliquots of ONS cells were used as the starting point for all the experiments described: phenotyping, gene and protein expression and functional assays. All cultures were grown under standard conditions on tissue culture plastic in DMEM/F12 supplemented with 10% FBS at 37°C and 5% CO_2. Frozen aliquots of ONS cells are available from the National Centre for Adult Stem Cell Research (http://www.griffith.edu.au/stem-cells), subject to patient consent, an appropriate Material Transfer Agreement, and payment of shipping and handling fees.

Flow cytometry

ONS cells were fixed in paraformaldehyde (4% in HBSS) for 10 minutes at room temperature (RT). Approximately 1×10^5 cells were washed twice with HBSS and incubated for 30 minutes at RT in 0.2 ml HBSS containing 1% BSA, 1% NGS and 0.1% Triton-X 100 together with the antibodies listed below. Cells were washed twice in HBSS-1%BSA and incubated for 30 minutes at RT with 1:400 dilution of the appropriate secondary antibody (below). After two washes, the cells were resuspended in washing buffer and analysed by flow cytometry (BD FACSAria flow cytometer). Isotype-matched controls were run in parallel for all antibodies. See supplementary material Table S5 for details of antigen, conjugate, dilution and supplier. Cells were considered immunopositive if their fluorescence was above the most fluorescent cells in the isotype-control sample. For each sample, the percentage of immunopositive cells was calculated and the groups were compared by Kruskal-Wallis one-way ANOVA because of unequal group variances. Dunn's multiple comparison tests were used to compare pairs of groups.

Gene expression profiling

Cell lines from 42 participants were grown in at least duplicate and profiled using the Illumina Beadarray Ref8v2 Chips, producing 88 gene expression profiles. Microarray data are available in the ArrayExpress database (http://www.ebi.ac.uk/arrayexpress) under accession number E-TABM-724. Cells expressed approximately 10,000 of the 22,185 transcripts represented by probes on the chips. The duplicates (biological replicates) for each cell line provided a quantitative measure of the reproducibility of the full process to generate the gene expression profile: cell culture, RNA

extraction and microarray hybridization. The correlation between the raw fluorescence values of biological replicates was extremely high (r^2>0.98 for all 42 cell lines), giving confidence that observed differences in gene expression among different cell lines were individual- and disease-associated and not due to technical factors.

ONS cells were grown until 80-90% confluent to assure similar growth phase and optimized mRNA yield. Total RNA was isolated using QIAGEN RNeasy Mini Kit using an on-column DNase I treatment. All RNA preparations were quantified using a Nanodrop ND1000 and checked with an Agilent 2100 Bioanalyser (RNA nano chips): only samples with RNA integrity number (RIN)>9 were accepted for RNA amplification. 500 ng of each RNA sample was amplified using the Ambion Illumina RNA Amplification Kit with biotin UTP labeling (Ambion, Inc.). Column-purified samples were subjected to in vitro transcription using T7 RNA polymerase for 4 hours to synthesize biotin-labeled cRNA. The cRNA was then column-purified prior to quantification of size and yield using an Agilent 2100 Bioanalyser. A total of 750 ng of cRNA was hybridized to human whole-genome Illumina Human-Refseq8 v2 BeadChips (Illumina, Inc.). These slides were scanned on an Illumina Beadstation and bead summarization was performed using BeadStudio Version 3.1.7 (Illumina, Inc.). After summarization, the raw data were exported from BeadStudio with no additional processing. The data from BeadStudio were imported into R/BioConductor using the readBead function from the BeadExplorer package (Elvidge, 2006). Background adjustment and quantile normalization (Bolstad et al., 2003) was performed using algorithms within the Affymetrix package (Gautier et al., 2004) (function: bg.adjust and normalize.quantiles). The normalized data were exported from R/BioConductor using write.beadData function for further analysis using Genespring GX 7.3.1. software (Agilent Technologies). Genes were initially filtered using Illumina detection score. The detection score represents the confidence that a given transcript is expressed above the control signal. A gene (probe) was included in further analysis if it had a detection score ≥0.99 in both biological replicate samples and in >25% of individuals within the disease group (PD, 5/19; SZ, 3/9) or the control group (4/19). This procedure generated a list of genes expressed in the cells. To determine genes that were differentially expressed in disease and control samples, the gene list was subjected to a parametric two-way ANOVA (P≤0.05) with disease status and replicate as main effects. The analysis was repeated for each disease compared with control. The P values were adjusted for multiple testing using the Benjamini and Hochberg false discovery rate method. The advantage of this analysis was the identification of genes whose expression was not altered with biological replicate, providing a list of genes that were differentially expressed in each disease compared with controls.

The lists of differentially expressed genes for each disease were then subjected to pathway 'over-representation' analysis using 'Ingenuity Pathway Analysis' (IPA) 6.0 (Ingenuity Systems, http://www.ingenuity.com). Over-representation is a measure of the probability that a gene list contains more members of a biochemical pathway than would be expected by chance, given the number of theoretical members in a pathway, the number of members in the list of genes of interest, and the number of genes used to generate the list of interest (i.e. the probes on the Illumina Ref8v2 BeadChip). This probability is determined by a right-tailed Fisher's exact test. The criterion for significance was α=0.01. Pathway analysis was also undertaken using the public database 'Database for Annotation, Visualization and Integrated Discovery' (DAVID) (Dennis et al., 2003). DAVID calculates a probability (EASE score) of genes of interest to be represented on pathways annotated by Kyoto Encyclopedia of Genes and Genomes (http://www.genome.jp/kegg/) or Biocarta (http://www.biocarta.com). The EASE score is calculated using the distribution of the Jackknife Fisher exact probability distribution, and provides a robust analysis of pathways. The criterion for significance was α=0.01.

qRT-PCR confirmation of gene expression

cDNA was synthesized from 2 μg of total RNA extracted from ONS cells using Superscript VILO cDNA Synthesis Kit (Invitrogen) according to the manufacturer's protocol. All qRT-PCR reactions were carried out using the commercial master mix Sensimix HRM with Evagreen dye (Quantace, UK). Reactions were performed on a RotorGene 6000 system (Corbett Technologies, Australia) using 5 μl of cDNA (1:10 dilution), and 0.5 μM of gene-specific primers to a total reaction volume of 15 μl. Cycling conditions were as follows: 10 minutes at 95°C followed by 40 cycles with denaturation for 15 seconds at 95°C, annealing for 10 seconds at 55-58°C and elongation for 10 seconds at 72°C. For annealing temperature and primer sequence see supplementary material Table S6. Melting curves were generated after each run to confirm a single PCR product. All reactions were performed in triplicate and in each run an internal standard curve were used to assign relative concentrations to the amplicons. All qRT-PCR primers were designed using ExPrimer (http://exprimer.ibab.ac.in) and Primer3 (http://frodo.wi.mit.edu/), and were synthesized by Sigma-Aldrich. Sequences and exon information used for primer design were obtained from public databases (GenBank, NCBI and Ensembl). BLAST searches were performed to confirm the total gene specificity of the primer sequences. Fluorescence data were converted into cycle threshold measurements using the RotorGene 6000 series software version 1.7. The data were analysed using REST 2008 software (http://www.gene-quantification.info/), where relative expression of target mRNA was normalized against EEF1A1 and quantified using a relative quantification approach with efficiency correction (Pfaffl, 2001; Pfaffl et al., 2002). EEF1A1 was chosen as it displayed the least variation within the microarray experiments. The data were compared statistically by pair-wise fixed reallocation randomization test (Pfaffl et al., 2002).

Protein expression profiling

Three ONS cell lines were selected from each group of control, PD and SZ samples. Cell lines used were: 100030003, 100030008 and 100070001 from the control group; 300020003, 300020004 and 300020005 from the SZ group; and 200050005, 200060005 and 200060007 from the PD group. Proteins extracted from these were subjected to 2D-DIGE to identify patient-control differences in protein expression. For each analysis, replicate gels were made from two protein samples from the same aliquot of cells and then each analysis was repeated on a second aliquot of cells grown independently. Reagents were sourced from GE Healthcare, UK (DIGE CyDyes, 2D Quant and 2D Cleanup Kits, urea, thiourea, CHAPS, DTT, Immobilized pH Gradient Strips), Fluka (Coomassie

G-250) and Sigma-Aldrich (CHCA matrix, ammonium bicarbonate, and peptide calibrants ACTH and angiotensin II).

ONS cells from confluent T175 flasks were washed with PBS and then resuspended in 0.5 ml of DIGE lysis buffer (7 M urea, 2 M thiourea, 4% CHAPS, 30 mM Tris). Samples were sonicated 3×10 seconds on ice with a Branson sonicator (output 2, constant) and centrifuged. Supernatant was transferred to new tubes and samples precipitated with a 2D Cleanup Kit (GE Healthcare) according to the manufacturer's instructions. Samples were resuspended in 50 µl of DIGE lysis buffer and pH checked (all approximately pH 8.5). Protein concentrations were determined using a 2D Quant Kit (GE Healthcare) according to the manufacturer's directions but halving all reaction volumes. DIGE labeling was performed using a CyDye DIGE Fluors minimal labeling kit (GE Healthcare) with minor modifications: for each sample 35 µg of protein was labeled with 400 pmol of Cy3 and (separately) Cy5 in a total volume of 20 µl. A pooled aliquot containing 38.5 µg of protein from each sample was bulk labeled with Cy2 using the same ratio of 35 µg of protein to 400 pmol of CyDye. Labeling was conducted on ice and in the dark for 30 minutes, and quenched by the addition of 10 mM lysine (1 µl) on ice for 10 minutes. Each sample was then diluted with an equal volume of 2× sample buffer (7 M urea, 2 M thiourea, 4% CHAPS, 80 mM DTT, 2% pharmalytes). Samples were then pooled as needed for 2D electrophoresis. Samples were further diluted to a final volume of 450 µl with rehydration buffer (7 M urea, 2 M thiourea, 4% CHAPS, 40 mM DTT, 1% pharmalytes) coloured with a trace amount of bromophenol blue. Immobilized pH gradient (IPGs) pH 3-11NL (24 cm) were actively rehydrated with samples at 30 V for 6 hours, followed by electrophoresis at 100 V for 2 hours, 500 V for 1 hour, 1000 V for 1 hour, 5000 V for 12 hours and 100 V for 4 hours in the dark. After isoelectric focusing, strips were equilibrated in 10 ml of equilibration buffer (75 mM Tris pH 8.8, 6 M urea, 30% v/v glycerol, 2% w/v SDS) for 15 minutes with 100 mg of DTT. Equilibration buffer with DTT was removed and replaced with 10 ml equilibration buffer containing 250 mg of iodoacetamide, and incubation was carried out for a further 15 minutes. After equilibration, strips were embedded on top of 24 cm large-format 12% SDS-PAGE gels with molten agarose (0.5% w/v agarose in 1× Laemmli running buffer coloured with a small amount of bromophenol blue). Second-dimension gels were electrophoresed in an Ettan DALT Twelve electrophoresis unit at 20°C with 3 watts/gel for 45 minutes followed by 10 watts/gel for 2 hours and then 20 watts/gel until the bromophenol blue dye front reached the bottom of the gel.

Gels were scanned with a Typhoon 9400 scanner (GE Healthcare) using predefined settings for Cy2, Cy3 and Cy5 dyes at 100 µm. Gel images were cropped as necessary and analysed using Progenesis SameSpots image-analysis program. Gels were aligned with autogenerated vectors, and then individually examined to confirm alignments, with additional vectors added where needed to improve alignments. Images were grouped based on disease status and comparison of SZ vs control and PD vs control conducted using a nested ANOVA analysis using normalized spot volumes. The criterion for significance was chosen as α=0.05 and a fold-change of at least 1.2. Further, protein spots were considered significant only if they fulfilled these criteria for duplicate analyses of gels from independently grown replicate cells.

Differentially expressed protein spots on the 2D-DIGE gels were identified using mass spectrometry. Preparative gels were prepared using pooled protein containing 67 µg of protein from each sample (600 µg total protein). Gels were electrophoresed as for DIGE-labeled material, but stained with Coomassie G-250 (0.1% w/v Coomassie G-250, 17% w/v ammonium sulphate, 34% methanol, 3% phosphoric acid). Coomassie-stained gels were scanned with an Odyssey infrared scanner (Li-Cor Biosciences, USA). Spots of interest were excized from gels, destained with 50% acetonitrile (ACN) plus 50 mM ammonium bicarbonate (ABC) and lyophilized in a speed vac. Gel pieces were rehydrated with 8 µl of trypsin (10 ng/µl in 50 mM ABC) at 4°C for 10 minutes. An additional 12 µl of 50 mM ABC buffer was added to gel pieces, and proteins digested overnight at 37°C. Peptides were extracted twice with 50% ACN plus 0.5% TFA, then concentrated in a speed vac and spotted to a MALDI-TOF target plate (0.4 µl) along with 0.4 µl of α-cyano-4-hydroxycinnamic acid (10 mg/ml in 50% ACN, 0.5% TFA) and allowed to dry. Spectra (500 shots) were collected using a Voyager DE STR MALDI-TOF mass spectrometer (Applied Biosystems, USA) in reflectron mode across 700-4000 m/z. An external calibration was performed using the peptides ACTH and angiotensin II.

Monoisotopic peak lists of calibrated spectra were generated using DataExplorer (Applied Biosystems) and searched in MASCOT accessed via the Australian Proteome Computational Facility (http://www.apcf.edu.au). Searches were conducted against all species, using a mass tolerance of ±0.5 Da, allowing for one miscleavage, carbamidomethylation as a fixed modification, and oxidized methionine as a variable modification. Only search results with a statistically significant score as determined by MASCOT were accepted as positive identifications of proteins.

Western analysis confirmation of protein expression

Protein samples were prepared from each cell line (5 µg total protein) and pooled to yield aliquots of 15 µg of total protein. Protein concentrations were determined using 2D Quant Kit (GE Healthcare). Samples were diluted 1:8 to yield three samples of identical volume and total protein concentration. Samples were serially diluted in ddH_2O and separated by SDS-PAGE (Cat#: NP0329BOX, Invitrogen, CA). Western blot analysis was performed by transferring protein samples onto PVDF membrane and probing with goat anti-transgelin-2 (Cat#: sc-51442, Santa Cruz Inc., CA) followed by detection with rabbit anti-goat IgG-HRP (Cat#: 61-1620, Invitrogen, CA) by using an ECL-Plus kit (GE Healthcare).

Cell function assays

ONS cells were grown in DMEM/F12 supplemented with 10% FBS, harvested using TrypLE Express (Invitrogen), washed in HBSS and resuspended in 10 ml of growth medium. Cell counts were performed using an automated particle counter (Beckman Coulter), cells were diluted to 2.5×10^4 cells/ml and 2500 cells (100 µl) were seeded into triplicate wells of 96-well plates [clear (absorbance-based), white (luminescence-based) or black (fluorescence-based) as appropriate, Nunc] and allowed to attach overnight. Medium was changed 24 hours prior to assay. All plates and reagents were equilibrated to RT prior to assay initiation and all results were obtained using a Synergy II plate reader (BioTek).

Reduced GSH content was determined using modified manufacturer-supplied protocols (GSH-Glo Glutathione Assay,

TRANSLATIONAL IMPACT

Clinical issue

There is an urgent need to develop new approaches for studying brain diseases to investigate the complex gene-environment interactions that contribute to their pathology. Schizophrenia (SZ), which is thought to be a disorder of brain development, is a life-long mental illness affecting ~1% of the world's population. Despite heritability being estimated at 80%, with family history the most important risk factor, genetic family and association studies have failed to reveal causative genes for the disease. Parkinson's disease (PD) is a degenerative neurological disorder affecting 0.1% of the world's population. Its prevalence is age-dependent, increasing to 2% of individuals over 60 years of age. This complex brain disease has genetic and environmental risk factors that impact mitochondrial function, oxidative stress and xenobiotic metabolism. Mutations in several genes cause inherited PD, although these account for <5% of cases. It is hoped that new approaches for studying brain diseases such as SZ and PD will reveal common steps in heterogeneous aetiological processes that could be targets for therapeutic intervention. Post-mortem brain samples provide some insights, but enable the identification of endpoints of disease only and are limited in supply. Other patient-derived cell types, such as fibroblasts and lymphoblastoid cell lines, are easily accessible but, because they are non-neural cells, they might lack important features necessary for understanding the biological bases of brain diseases.

Results

In this paper, the authors present a new patient-cell-based model for investigating brain diseases. They derive and culture cells from the olfactory mucosa, the sense organ of smell, which contains stem cells that continually regenerate the organ's sensory neurons throughout adult life. The authors use this model to identify the genes, proteins and cellular functions that are altered in cells derived from patients with SZ and PD by comparing them with cells derived from healthy controls. This approach demonstrates disease-specific differences in gene expression, protein expression and cell function that are in line with current theories regarding the aetiologies of SZ and PD. In cells derived from patients with SZ, the authors identify dysregulation in cell signalling pathways of brain development, some of which have previously been identified as candidates for disease susceptibility (such as Reelin signalling, VDR/RXR activation, IL-8 signalling, glutathione metabolism and ErbB signalling). Importantly, fibroblasts derived from patients with SZ did not show these differences. In cells derived from patients with PD, the authors identify marked changes in signalling pathways involved in oxidative stress and xenobiotic metabolism (such as the NRF2-mediated oxidative stress response, aryl hydrocarbon receptor signalling, glutathione metabolism and xenobiotic metabolism signalling). Furthermore, the authors uncover new specific molecular and genetic pathways that might expand our understanding of disease aetiology and advance therapeutic development.

Implications and future directions

The capacity to tease out disease-specific differences using this patient-cell-based model provides specific candidate genes and cell pathways for future studies of brain diseases. In addition to providing informative data on SZ and sporadic PD, this model might be useful for studying the cellular and molecular bases of other neurological conditions. This system can be applied to improve our understanding of disease aetiology, the development of new diagnostics and drug discovery.

doi:10.1242/dmm.006171

Promega). Medium was aspirated and cells washed twice in HBSS (100 µl per well), then 50 µl of` GSH reaction buffer was added to each well and plates were incubated at RT for 15 minutes, light protected. Luciferin detection reagent (50 µl) was added and following a further 15 minutes light-protected incubation, luminescence intensity was recorded. MTS reagent was prepared according to manufacturer-supplied protocols (CellTiter aqueous MTS assay protocol, Promega), and 20 µl of prepared reagent added to each well. After incubation for 2 hours at 37°C, absorbance at 490 nm was recorded. Chymotrypsin-like proteasome activities were measured using the supplied protocol (Cell-Based Proteasome-Glo Assays, Promega). Briefly, cells were washed twice in HBSS and left in 50 µl of HBSS, and 50 µl of prepared reagent was added to each well. After incubation for 10 minutes at RT, luminescence intensity was recorded. ATP levels were measured according to manufacturer-supplied protocols (ATPlite assay kit, Perkin Elmer). Culture medium was aspirated, and the cells were washed twice in HBSS and subsequently left in 100 µl of HBSS. Lysis buffer (50 µl) was added to each well and the plate incubated at RT for 10 minutes, after which luciferin substrate (50 µl) was added. Following a further incubation at RT for 10 minutes, luminescence intensity was recorded. Lactate dehydrogenase activity was measured using manufacturer-supplied protocols (CytoTox-ONE Homogenous Membrane Integrity Assay, Promega) by addition of 100 µl of prepared reagent to each well. After incubation at RT for 1 hour, each well was excited at 560 nm and intensity of fluorescence emitted at 590 nm was recorded. Caspase-3/7 activity was measured according to manufacturer-supplied protocols (Apo-ONE Homogenous Caspase-3/7 Assay, Promega) via addition of 100 µl of freshly prepared reagent directly to the culture medium. After incubation for 2 hours at RT, each well was excited at 485 nm and intensity of fluorescence emitted at 530 nm was recorded.

For all assays, background signal was determined by including triplicate wells containing only growth medium in parallel, and the resulting average background reading was subtracted from all other values for each assay. Data were normalized to DNA content, determined using supplied protocols (CyQUANT-NF, Invitrogen; 50 µl of prepared reagent per well, including medium-only control wells). For each cell line, triplicate values from each assay were averaged and a signal:DNA content ratio determined. Statistical analysis was conducted using a two-tailed unpaired *t*-test (GraphPad Prism 5 for Windows) on pooled data from repeated experiments in which each cell line was assayed in triplicate.

ACKNOWLEDGEMENTS

We thank Amanda Miotto and Othmar Korn for database infrastructure support. This research was supported by a grant to A.M.-S. from the Australian Department of Health and Ageing. Bioinformatic analysis was supported by Queensland Government Smart Futures Fund.

COMPETING INTERESTS

The authors declare no competing financial interests.

AUTHOR CONTRIBUTIONS

N.M., G.A., R.S, A.M.V., A.L.C., A.N., B.B., M.B., R.C., J.C., Y.F., F.F., R.M., J.M., W.M., C.P., J.R., S.R., P.S. and C.S. designed and performed the experiments. N.M., G.A., A.L.C., A.M.V, A.N., J.A., M.A., A.B., A.M.C., G.S., S.M., G.M., S.A.W., C.W. and A.M.-S. performed the analyses. A.M.-S. conceived the project and coordinated manuscript preparation. All authors contributed to and edited the manuscript.

SUPPLEMENTARY MATERIAL

Supplementary material for this article is available at http://dmm.biologists.org/lookup/suppl/doi:10.1242/dmm.005447/-/DC1

Received 26 January 2010; Accepted 19 May 2010.

REFERENCES

Abrams, M. T., Kaufmann, W. E., Rousseau, F., Oostra, B. A., Wolozin, B., Taylor, C. V., Lishaa, N., Morel, M. L., Hoogeveen, A. and Reiss, A. L. (1999). FMR1 gene expression in olfactory neuroblasts from two males with fragile X syndrome. *Am. J. Med. Genet.* **82**, 25-30.

Arnold, S. E., Han, L. Y., Moberg, P. J., Turetsky, B. I., Gur, R. E., Trojanowski, J. Q. and Hahn, C. G. (2001). Dysregulation of olfactory receptor neuron lineage in schizophrenia. *Arch. Gen. Psychiatry* **58**, 829-835.

Aston, C., Jiang, L. and Sokolov, B. P. (2004). Microarray analysis of postmortem temporal cortex from patients with schizophrenia. *J. Neurosci. Res* **77**, 858-866.

Benmoyal-Segal, L. and Soreq, H. (2006). Gene-environment interactions in sporadic Parkinson's disease. *J. Neurochem.* **97**, 1740-1755.

Bolstad, B. M., Irizarry, R. A., Astrand, M. and Speed, T. P. (2003). A comparison of normalization methods for high density oligonucleotide array data based on variance and bias. *Bioinformatics* **19**, 185-193.

Brewer, W. J., Wood, S. J., McGorry, P. D., Francey, S. M., Phillips, L. J., Yung, A. R., Anderson, V., Copolov, D. L., Singh, B., Velakoulis, D. et al. (2003). Impairment of olfactory identification ability in individuals at ultra-high risk for psychosis who later develop schizophrenia. *Am. J. Psychiatry* **160**, 1790-1794.

Brown, A. S. (2006). Prenatal infection as a risk factor for schizophrenia. *Schizophr. Bull.* **32**, 200-202.

Brown, A. S., Hooton, J., Schaefer, C. A., Zhang, H., Petkova, E., Babulas, V., Perrin, M., Gorman, J. M. and Susser, E. S. (2004). Elevated maternal interleukin-8 levels and risk of schizophrenia in adult offspring. *Am. J. Psychiatry* **161**, 889-895.

Castle, D. J., Jablensky, A., McGrath, J. J., Carr, V., Morgan, V., Waterreus, A., Valuri, G., Stain, H., McGuffin, P. and Farmer, A. (2006). The diagnostic interview for psychoses (DIP): development, reliability and applications. *Psychol. Med.* **36**, 69-80.

Chen, X., Fang, H. and Schwob, J. E. (2004). Multipotency of purified, transplanted globose basal cells in olfactory epithelium. *J. Comp. Neurol.* **469**, 457-474.

Colantuoni, C., Hyde, T. M., Mitkus, S., Joseph, A., Sartorius, L., Aguirre, C., Creswell, J., Johnson, E., Deep-Soboslay, A., Herman, M. M. et al. (2008). Age-related changes in the expression of schizophrenia susceptibility genes in the human prefrontal cortex. *Brain Struct. Funct.* **213**, 255-271.

Corfas, G., Roy, K. and Buxbaum, J. D. (2004). Neuregulin 1-erbB signaling and the molecular/cellular basis of schizophrenia. *Nat. Neurosci.* **7**, 575-580.

Cuadrado, A., Moreno-Murciano, P. and Pedraza-Chaverri, J. (2009). The transcription factor Nrf2 as a new therapeutic target in Parkinson's disease. *Expert Opin. Ther. Targets* **13**, 319-329.

Delorme, B., Nivet, E., Gaillard, J., Haupl, T., Ringe, J., Deveze, A., Magnan, J., Sohier, J., Khrestchatisky, M., Roman, F. S. et al. (2010). The human nose harbours a niche of olfactory ectomesenchymal stem cells displaying neurogenic and osteogenic properties. *Stem Cells Dev*. **19**, 853-866.

Denison, M. S. and Nagy, S. R. (2003). Activation of the aryl hydrocarbon receptor by structurally diverse exogenous and endogenous chemicals. *Annu. Rev. Pharmacol. Toxicol.* **43**, 309-334.

Dennis, G., Jr, Sherman, B. T., Hosack, D. A., Yang, J., Gao, W., Lane, H. C. and Lempicki, R. A. (2003). DAVID: Database for Annotation, Visualization, and Integrated Discovery. *Genome Biol.* **4**, P3.

Doty, R. L. (2009). The olfactory system and its disorders. *Semin. Neurol.* **29**, 74-81.

Elvidge, G. (2006). BeadExplorer: QC, normalisation, annotation and exploration of Illumina BeadChip data. R package version 1.2.0. http://bioconductor.org/packages/1.9/bioc/vignettes/BeadExplorer/inst/doc/BeadHelp.pdf.

Erdely, H. A., Tamminga, C. A., Roberts, R. C. and Vogel, M. W. (2006). Regional alterations in RGS4 protein in schizophrenia. *Synapse* **59**, 472-479.

Eyles, D., Brown, J., Mackay-Sim, A., McGrath, J. and Feron, F. (2003). Vitamin D3 and brain development. *Neuroscience* **118**, 641-653.

Fatemi, S. H., Kroll, J. L. and Stary, J. M. (2001). Altered levels of Reelin and its isoforms in schizophrenia and mood disorders. *NeuroReport* **12**, 3209-3215.

Féron, F., Perry, C., McGrath, J. J. and Mackay-Sim, A. (1998). New techniques for biopsy and culture of human olfactory epithelial neurons. *Arch. Otolaryngol. Head Neck Surg.* **124**, 861-866.

Féron, F., Perry, C., Hirning, M. H., McGrath, J. and Mackay-Sim, A. (1999). Altered adhesion, proliferation and death in neural cultures from adults with schizophrenia. *Schizophr. Res.* **40**, 211-218.

Feron, F., Burne, T. H., Brown, J., Smith, E., McGrath, J. J., Mackay-Sim, A. and Eyles, D. W. (2005). Developmental Vitamin D3 deficiency alters the adult rat brain. *Brain Res. Bull.* **65**, 141-148.

Gautier, L., Cope, L., Bolstad, B. M. and Irizarry, R. A. (2004). affy – analysis of Affymetrix GeneChip data at the probe level. *Bioinformatics* **20**, 307-315.

Goodman, A. B. (1998). Three independent lines of evidence suggest retinoids as causal to schizophrenia. *Proc. Natl. Acad. Sci. USA* **95**, 7240-7244.

Guidotti, A., Auta, J., Davis, J. M., Di-Giorgi-Gerevini, V., Dwivedi, Y., Grayson, D. R., Impagnatiello, F., Pandey, G., Pesold, C., Sharma, R. et al. (2000). Decrease in reelin and glutamic acid decarboxylase67 (GAD67) expression in schizophrenia and bipolar disorder: a postmortem brain study. *Arch. Gen. Psychiatry* **57**, 1061-1069.

Haehner, A., Boesveldt, S., Berendse, H. W., Mackay-Sim, A., Fleischmann, J., Silburn, P. A., Johnston, A. N., Mellick, G. D., Herting, B., Reichmann, H. et al. (2009). Prevalence of smell loss in Parkinson's disease-a multicenter study. *Parkinsonism Relat. Disord.* **15**, 490-494.

Hakak, Y., Walker, J. R., Li, C., Wong, W. H., Davis, K. L., Buxbaum, J. D., Haroutunian, V. and Fienberg, A. A. (2001). Genome-wide expression analysis reveals dysregulation of myelination-related genes in chronic schizophrenia. *Proc. Natl. Acad. Sci. USA* **98**, 4746-4751.

Harrison, P. J. (1999). The neuropathology of schizophrenia. A critical review of the data and their interpretation. *Brain* **122**, 593-624.

Henchcliffe, C. and Beal, M. F. (2008). Mitochondrial biology and oxidative stress in Parkinson disease pathogenesis. *Nat. Clin. Pract. Neurol.* **4**, 600-609.

Hiesberger, T., Trommsdorff, M., Howell, B. W., Goffinet, A., Mumby, M. C., Cooper, J. A. and Herz, J. (1999). Direct binding of Reelin to VLDL receptor and ApoE receptor 2 induces tyrosine phosphorylation of disabled-1 and modulates tau phosphorylation. *Neuron* **24**, 481-489.

Hoepken, H. H., Gispert, S., Azizov, M., Klinkenberg, M., Ricciardi, F., Kurz, A., Morales-Gordo, B., Bonin, M., Riess, O., Gasser, T. et al. (2008). Parkinson patient fibroblasts show increased alpha-synuclein expression. *Exp. Neurol.* **212**, 307-313.

Impagnatiello, F., Guidotti, A. R., Pesold, C., Dwivedi, Y., Caruncho, H., Pisu, M. G., Uzunov, D. P., Smalheiser, N. R., Davis, J. M., Pandey, G. N. et al. (1998). A decrease of reelin expression as a putative vulnerability factor in schizophrenia. *Proc. Natl. Acad. Sci. USA* **95**, 15718-15723.

Jenner, P. (2008). Functional models of Parkinson's disease: a valuable tool in the development of novel therapies. *Ann. Neurol.* **64**, S16-S29.

Kozlovsky, N., Belmaker, R. H. and Agam, G. (2000). Low GSK-3beta immunoreactivity in postmortem frontal cortex of schizophrenic patients. *Am. J. Psychiatry* **157**, 831-833.

Kozlovsky, N., Regenold, W. T., Levine, J., Rapoport, A., Belmaker, R. H. and Agam, G. (2004). GSK-3beta in cerebrospinal fluid of schizophrenia patients. *J. Neural. Transm.* **111**, 1093-1098.

LaMantia, A. S. (1999). Forebrain induction, retinoic acid, and vulnerability to schizophrenia: insights from molecular and genetic analysis in developing mice. *Biol. Psychiatry* **46**, 19-30.

Lesage, S. and Brice, A. (2009). Parkinson's disease: from monogenic forms to genetic susceptibility factors. *Hum. Mol. Genet.* **18**, R48-R59.

Leung, C. T., Coulombe, P. A. and Reed, R. R. (2007). Contribution of olfactory neural stem cells to tissue maintenance and regeneration. *Nat. Neurosci.* **10**, 720-726.

Lewis, D. A. and Levitt, P. (2002). Schizophrenia as a disorder of neurodevelopment. *Ann. Rev. Neurosci.* **25**, 409-432.

Lovestone, S., Killick, R., Di Forti, M. and Murray, R. (2007). Schizophrenia as a GSK-3 dysregulation disorder. *Trends Neurosci.* **30**, 142-149.

Mackay-Sim, A. and Kittel, P. (1991). Cell dynamics in the adult mouse olfactory epithelium: a quantitative autoradiographic study. *J. Neurosci.* **11**, 979-984.

Mackay-Sim, A. and Silburn, P. (2008). Stem cells and genetic disease. *Cell Prolif.* **41**, 85-93.

Mahadik, S. P. and Mukherjee, S. (1996). Cultured skin fibroblasts as a cell model for investigating schizophrenia. *J. Psychiatr. Res.* **30**, 421-439.

Marenco, S. and Weinberger, D. R. (2000). The neurodevelopmental hypothesis of schizophrenia: following a trail of evidence from cradle to grave. *Dev. Psychopathol.* **12**, 501-527.

Martinez, A. and Soriano, E. (2005). Functions of ephrin/Eph interactions in the development of the nervous system: emphasis on the hippocampal system. *Brain Res. Brain Res. Rev.* **49**, 211-226.

Mateizel, I., De Temmerman, N., Ullmann, U., Cauffman, G., Sermon, K., Van de Velde, H., De Rycke, M., Degreef, E., Devroey, P., Liebaers, I. et al. (2006). Derivation of human embryonic stem cell lines from embryos obtained after IVF and after PGD for monogenic disorders. *Hum. Reprod.* **21**, 503-511.

Matigian, N. A., McCurdy, R. D., Feron, F., Perry, C., Smith, H., Filippich, C., McLean, D., McGrath, J., Mackay-Sim, A., Mowry, B. et al. (2008). Fibroblast and lymphoblast gene expression profiles in schizophrenia: are non-neural cells informative? *PLoS ONE* **3**, e2412.

McCurdy, R. D., Feron, F., Perry, C., Chant, D. C., McLean, D., Matigian, N., Hayward, N. K., McGrath, J. J. and Mackay-Sim, A. (2006). Cell cycle alterations in biopsied olfactory neuroepithelium in schizophrenia and bipolar I disorder using cell culture and gene expression analyses. *Schizophr. Res.* **82**, 163-173.

McGrath, J., Eyles, D., Mowry, B., Yolken, R. and Buka, S. (2003a). Low maternal vitamin D as a risk factor for schizophrenia: a pilot study using banked sera. *Schizophr. Res.* **63**, 73-78.

McGrath, J. J., Feron, F. P., Burne, T. H., Mackay-Sim, A. and Eyles, D. W. (2003b). The neurodevelopmental hypothesis of schizophrenia: a review of recent developments. *Ann. Med.* **35**, 86-93.

McGrath, J., Saari, K., Hakko, H., Jokelainen, J., Jones, P., Jarvelin, M. R., Chant, D. and Isohanni, M. (2004). Vitamin D supplementation during the first year of life and risk of schizophrenia: a Finnish birth cohort study. *Schizophr. Res.* **67**, 237-245.

McNaught, K. S. and Olanow, C. W. (2006). Protein aggregation in the pathogenesis of familial and sporadic Parkinson's disease. *Neurobiol. Aging* **27**, 530-545.

Mellick, G. D. (2006). CYP450, genetics and Parkinson's disease: gene x environment interactions hold the key. *J. Neural Transm.* **2006**, 159-165.
Mirnics, K., Middleton, F. A., Stanwood, G. D., Lewis, D. A. and Levitt, P. (2001). Disease-specific changes in regulator of G-protein signaling 4 (RGS4) expression in schizophrenia. *Mol. Psychiatry* **6**, 293-301.
Miyamae, Y., Nakamura, Y., Kashiwagi, Y., Tanaka, T., Kudo, T. and Takeda, M. (1998). Altered adhesion efficiency and fibronectin content in fibroblasts from schizophrenic patients. *Psychiatry Clin. Neurosci.* **52**, 345-352.
Murrell, W., Bushell, G. R., Livesey, J., McGrath, J., MacDonald, K. P. A., Bates, P. R. and Mackay-Sim, A. (1996). Neurogenesis in adult human. *NeuroReport* **7**, 1189-1194.
Murrell, W., Feron, F., Wetzig, A., Cameron, N., Splatt, K., Bellette, B., Bianco, J., Perry, C., Lee, G. and Mackay-Sim, A. (2005). Multipotent stem cells from adult olfactory mucosa. *Dev. Dyn.* **233**, 496-515.
Murrell, W., Wetzig, A., Donnellan, M., Feron, F., Burne, T., Meedeniya, A., Kesby, J., Bianco, J., Perry, C., Silburn, P. et al. (2008). Olfactory mucosa is a potential source for autologous stem cell therapy for Parkinson's disease. *Stem Cells* **26**, 2183-2192.
Murrell, W., Sanford, E., Anderberg, L., Cavanagh, B. and Mackay-Sim, A. (2009). Olfactory stem cells can be induced to express chondrogenic phenotype in a rat intervertebral disc injury model. *Spine J.* **9**, 585-594.
Nie, L., Wu, G. and Zhang, W. (2006). Correlation between mRNA and protein abundance in Desulfovibrio vulgaris: a multiple regression to identify sources of variations. *Biochem. Biophys. Res. Commun.* **339**, 603-610.
Othman, M., Lu, C., Klueber, K., Winstead, W. and Roisen, F. (2005). Clonal analysis of adult human olfactory neurosphere forming cells. *Biotech. Histochem.* **80**, 189-200.
Park, I. H., Arora, N., Huo, H., Maherali, N., Ahfeldt, T., Shimamura, A., Lensch, M. W., Cowan, C., Hochedlinger, K. and Daley, G. Q. (2008). Disease-specific induced pluripotent stem cells. *Cell* **134**, 877-886.
Pascal, L. E., True, L. D., Campbell, D. S., Deutsch, E. W., Risk, M., Coleman, I. M., Eichner, L. J., Nelson, P. S. and Liu, A. Y. (2008). Correlation of mRNA and protein levels: cell type-specific gene expression of cluster designation antigens in the prostate. *BMC Genomics* **9**, 246.
Pfaffl, M. W. (2001). A new mathematical model for relative quantification in real-time RT-PCR. *Nucleic Acids Res.* **29**, e45.
Pfaffl, M. W., Horgan, G. W. and Dempfle, L. (2002). Relative expression software tool (REST) for group-wise comparison and statistical analysis of relative expression results in real-time PCR. *Nucleic Acids Res.* **30**, e36.
Raedler, T. J., Knable, M. B. and Weinberger, D. R. (1998). Schizophrenia as a developmental disorder of the cerebral cortex. *Curr. Opin. Neurobiol.* **8**, 157-161.
Roisen, F. J., Klueber, K. M., Lu, C. L., Hatcher, L. M., Dozier, A., Shields, C. B. and Maguire, S. (2001). Adult human olfactory stem cells. *Brain Res.* **890**, 11-22.
Ronnett, G. V., Leopold, D., Cai, X., Hoffbuhr, K. C., Moses, L., Hoffman, E. P. and Naidu, S. (2003). Olfactory biopsies demonstrate a defect in neuronal development in Rett's syndrome. *Ann. Neurol.* **54**, 206-218.
Schmid, R. S., Jo, R., Shelton, S., Kreidberg, J. A. and Anton, E. S. (2005). Reelin, integrin and DAB1 interactions during embryonic cerebral cortical development. *Cereb. Cortex* **15**, 1632-1636.
Summers, K. M. (1996). Relationship between genotype and phenotype in monogenic diseases: relevance to polygenic diseases. *Hum. Mutat.* **7**, 283-293.
Sutherland, G. T., Matigian, N. A., Chalk, A. M., Anderson, M. J., Silburn, P. A., Mackay-Sim, A., Wells, C. A. and Mellick, G. D. (2009). A cross-study transcriptional analysis of Parkinson's disease. *PLoS ONE* **4**, e4955.
Tkachev, D., Mimmack, M. L., Ryan, M. M., Wayland, M., Freeman, T., Jones, P. B., Starkey, M., Webster, M. J., Yolken, R. H. and Bahn, S. (2003). Oligodendrocyte dysfunction in schizophrenia and bipolar disorder. *Lancet* **362**, 798-805.
Trommsdorff, M., Gotthardt, M., Hiesberger, T., Shelton, J., Stockinger, W., Nimpf, J., Hammer, R. E., Richardson, J. A. and Herz, J. (1999). Reeler/Disabled-like disruption of neuronal migration in knockout mice lacking the VLDL receptor and ApoE receptor 2. *Cell* **97**, 689-701.
Turetsky, B. I., Hahn, C. G., Borgmann-Winter, K. and Moberg, P. J. (2009). Scents and nonsense: olfactory dysfunction in schizophrenia. *Schizophr. Bull.* **35**, 1117-1131.
Verlinsky, Y., Strelchenko, N., Kukharenko, V., Rechitsky, S., Verlinsky, O., Galat, V. and Kuliev, A. (2005). Human embryonic stem cell lines with genetic disorders. *Reprod. Biomed. Online* **10**, 105-110.
Wang, L., Lockstone, H. E., Guest, P. C., Levin, Y., Palotas, A., Pietsch, S., Schwarz, E., Rahmoune, H., Harris, L. W., Ma, D. et al. (2009). Expression profiling of fibroblasts identifies cell cycle abnormalities in schizophrenia. *J. Proteome Res.* **9**, 521-527.
Winkler-Stuck, K., Wiedemann, F. R., Wallesch, C. W. and Kunz, W. S. (2004). Effect of coenzyme Q(10) on the mitochondrial function of skin fibroblasts from Parkinson patients. *J. Neurol. Sci.* **220**, 41-48.
Wolozin, B., Zheng, B., Loren, D., Lesch, K. P., Lebovics, R. S., Lieberburg, I. and Sunderland, T. (1992a). Beta/A4 domain of APP: antigenic differences between cell lines. *J. Neurosci. Res.* **33**, 189-195.
Wolozin, B., Sunderland, T., Zheng, B. B., Resau, J., Dufy, B., Barker, J., Swerdlow, R. and Coon, H. (1992b). Continuous culture of neuronal cells from adult human olfactory epithelium. *J. Mol. Neurosci.* **3**, 137-146.
Wray, N. R., Goddard, M. E. and Visscher, P. M. (2008). Prediction of individual genetic risk of complex disease. *Curr. Opin. Genet. Dev.* **18**, 257-263.
Zaidel-Bar, R., Itzkovitz, S., Ma'ayan, A., Iyengar, R. and Geiger, B. (2007). Functional atlas of the integrin adhesome. *Nat. Cell Biol.* **9**, 858-867.